INVESTIGATIONS OF CARBON AND WATER FLUXES IN A SIERRA NEVADA MEADOW

Darren Blackburn, Andrew Oliphant, Shamim Mousavi, Jerry Davis
San Francisco State University, Department of Geography & Environment

INTRODUCTION

Mountain meadows are important niche ecosystems that provide a number of services that support diverse plant, wildlife and human communities throughout the broader watershed. These benefits include improving water quality, moderating runoff and acting as biodiversity hotspots (Loheide et al. 2009). Historic and current land use in the Sierra Nevada (SN) have contributed to major watershed degradation and negatively affected the ability of montane meadows to function as rich and diverse ecosystems (Viers et al. 2013). Grazing animals are considered to be a primary source of land use that have a negative impact on SN meadows but logging and mining have also been identified (Viers et al. 2013). Degradation of meadows is associated with stream channel incision, which effectively lowers the water table. A high water table is required to support the sedges, grasses and herbs that naturally occur in these systems and if natural flow patterns are not maintained, dryland shrubs and grass species have the potential to encroach and dominate the ecosystem (Viers et al. 2013). Given the large growth cycle in healthy meadows, it is also expected that they sequester a large amount of carbon, support organic soils and enhance humidity through evapotranspiration, but relatively little work has been done on the carbon and water cycles of these sensitive ecosystems.

RESEARCH OBJECTIVE

To investigate ecosystem-atmosphere CO_2 exchanges in a meadow ecosystem in the northern Sierra Nevada. In particular the study aims to assess diurnal, seasonal and synoptic controls on the net CO_2 exchange (NEE), the gross primary production (GPP), ecosystem evapotranspiration (ET) and ecosystem respiration (Re).

STUDY SITE

Loney Meadow, located at nearly 2,000 m in the Tahoe National Forest, has been identified as a degraded meadow and is scheduled to undergo restoration work to raise the water table in 2017. The area of the meadow is approximately 138,307 m^2 and it is actively grazed by cattle between June and September. Texas Creek flows through the meadow, which is part of the Yuba River watershed.

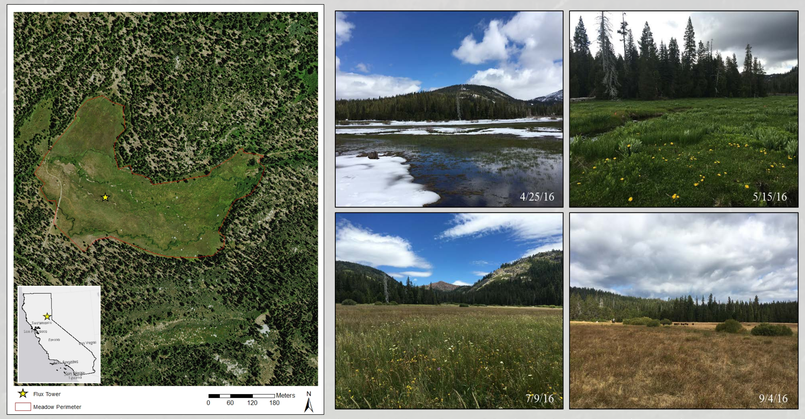

Fig. 1 Site map (left) and images with dates taken during site visits to Loney Meadow (right). See reference for map sources.

METHODS

A micrometeorological tower with eddy covariance (EC) instruments was deployed at the site for most of the snow-free period from May 16 to September 9, 2016. The measurements include: fluxes of CO_2, water vapor, surface radiation and energy budget components; ancillary meteorological and soil data; and an automated camera capturing daily images of the meadow surface. The sampling frequency was 10 Hz for eddy covariance block averages on a 30-minute basis. EC data that did not meet the following quality control requirements was rejected:

1) Low friction velocity of <0.2 m/s
2) Values that were outside plausible limits or spikes
3) Source area of flux data was not within 90% of the meadow boundary (modeled for each 30-min period)

Fig. 2 Table of equipment (left) and image of the flux tower deployed at Loney Meadow (right).

Instrument	Type	Variable(s) Measured	Units	Measurement Height
Thermistor (a.) Hygristor (a.)	HMP45C: Visala	Air Temperature / Relative Humidity	°C / %	2.44 m
Sonic Anemometer (b.)	CSAT3 3D: Campbell Scientific Inc.	3D Wind Speed / Sonic Temperature	m/s / °C	2.44 m
Infrared Gas Analyzer (c.)	7500: LI-COR Inc.	CO_2 / Water Vapor	mgC m^{-2} s^{-1} / gH_2O m^{-2} s^{-1}	2.44 m
Pyranometer (d.) Pyrgeometer (d.)	NR01: HukseFlux Inc.	Shortwave Radiation Longwave Radiation	W m^{-2}	1.25 m
Heat Flux Plates (e.) (2)	HFP01: HukseFlux Inc.	Ground Heat Flux	W m^{-2}	-5 cm
Soil Temperature Thermistor (e.)	CS107: Campbell Scientific Inc.	Soil Temperature	°C	Tg1: -2 (cm) Tg2: -10 (cm)
Ground Thermocouples (e.)	E Type: Omega	Soil Temperature	°C	-1 & -2.5 cm
Soil Moisture Probe (e.)	CS616: Campbell Scientific Inc.	Volumetric Water Content	m^3 m^{-3}	-1: -10 cm
Rain Gauge	TR-5251: Texas Electronics	Precipitation	mm	43 (cm)

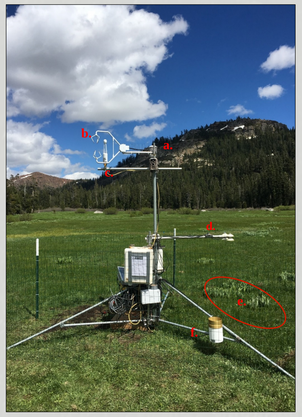

RESULTS: 1. Seasonal patterns in ecosystem CO_2 fluxes and environ. drivers

Fig. 3 (a) Daily total CO_2 exchanges between the ecosystem and atmosphere throughout the growing season, including gross primary production (GPP), Respiration (Re) and net ecosystem exchange of CO_2 (NEE) and environmental controls including (in descending order) daily average photosynthetically active radiation (PAR) (b), air/soil temperature anddaily total precipitation (c) and soil moisture (d). (Top) Selected images of meadow surface (west facing) taken from the top of flux tower and approximation of distinct phases of the growing seasons divided into four periods. Gap filling of rejected EC data was accomplished through modeling Re based on soil temperature and GPP based on seasonal light use efficiency.

The seasonal pattern of GPP closely mirrored that of NEE indicating that it was the driving component of seasonal variability of the CO_2 flux. GPP plateaued between June 5 and July 6 (Period 2), the time in the growing season when leaf area index (LAI) had reached its maximum and soil moisture remained high (above 0.4 m^{-3} m^{-3}). Re showed much less variability than GPP remaining between 17 and 27 gC m^{-2} d^{-1} throughout most of the study period. On a daily basis, PAR appears to be the primary driver of the fluctuating pattern of GPP (Fig. 3a & 3b). However, according to the LUE analysis shown below, that relationship weakens as vegetation senesces. A sharp decline in soil moisture from about Day 171 appears to be the main driver of this the onset of Period 3 where GPP began to decline (Fig. 3a, d). This reduction in soil moisture had little effect on Re observed. On August 8 the meadow ecosystem switched from a net sink of CO_2 to a weak source. On a seasonal basis, declining soil moisture levels appear to be the main environmental driver that controls the larger seasonal trends as they relate to declining productivity and vegetation senescence.

2. Seasonal phases of carbon fluxes and light use efficiency

TIME PERIOD (Day of Year)	GPP (gC m^{-2} d^{-1})	RE (gC m^{-2} d^{-1})	NEE (gC m^{-2} d^{-1})
Period 1 (138 – 157) May 17 - June 5	34.6	18.09	-13.65
Period 2 (158 – 187) June 6 - July 5	43.65	22.41	-18.51
Period 3 (188 – 220) July 6 - August 7	31.74	23.35	-5.48
Period 4 (221 – 250) August 8 - September 6	19.66	21.35	2.97
Total Study Period (138 - 157)	32.48	22.10	-7.71

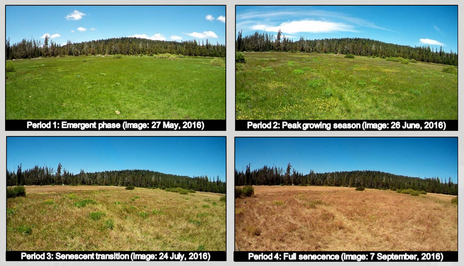

Fig. 4. (left) Table showing average daily total CO_2 flux magnitudes for each seasonal period and the entire study period. Images (right) show the meadow ecosystem near the middle of each seasonal period.

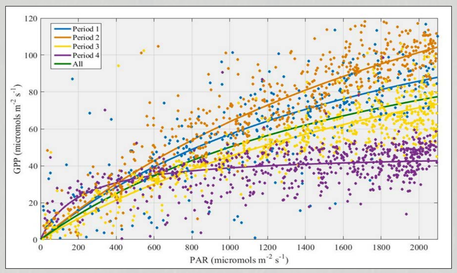

Seasonal Period	α	A_{max}	R^2	n	Average GPP (mgC m^{-2} s^{-1})
ALL	0.0741	154.3	0.41	2548	0.704
1	0.0849	173.7	0.57	411	0.774
2	0.0861	246.7	0.82	718	0.91
3	0.0609	172.9	0.67	766	0.685
4	0.223	47	0.08	637	0.454

Fig. 5. LUE curves fit to rectangular hyperbola curves for different seasonal periods (left), based on 30-minute average flux values during daytime. Curve parameters and statistics are provided in the table (right).

The high α and A_{max} values for Periods 1 and 2 indicate a strong response to light until the vegetation begins to senesce during the late summer and fall months, when the latter declines with a very low level of saturation and photosynthesis overall. With an R^2 value of 0.82, data from Period 2 is most closely fit to the regression curve during the study period. Period 4 also shows by far the weakest correlation (R^2 = 0.08) between GPP and PAR.

3. Evapotranspiration and water use efficiency

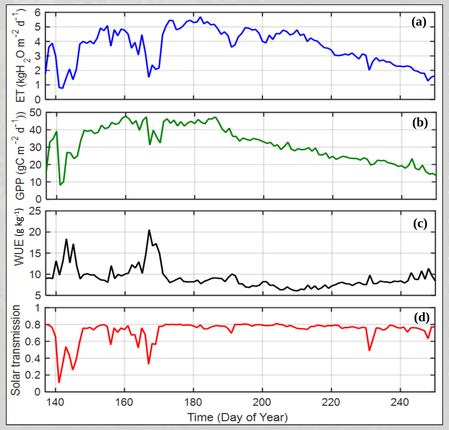

Fig. 6 Daily total fluxes of (a) evapotranspiration (ET) and (b) ecosystem gross primary ecosystem (GPP), with daily ratios of (c) water use efficiency (WUE=GPP/ET, g kg^{-1}) and (d) solar transmission (surface observed solar radiation divided by modeled extraterrestrial solar radiation for the same place and time).

Evapotranspiration closely follows the seasonal patterns of GPP, indicating the strong dominance of transpiration in ET during the growing season. This also produces a fairly consistent water use efficiency estimate of between about 5 and 10 g kg^{-1}, fairly low by global ecosystem standards. The marked differences occur during cloudy periods, indicated by low solar transmission, when WUE approximately doubles. Although this produces a decline in both driving variables, light use efficiency is higher under diffuse light conditions reducing the decline in GPP, while vapor pressure deficit also declines, enhancing the reduction in transpiration, relative to GPP.

4. Diurnal Patterns in ecosystem functioning

The diurnal pattern of GPP was near symmetrical in all four seasonal periods (Fig. 7). Period 3 exhibited a much lower peak of GPP, explained by declining soil moisture and higher vapor pressure deficit. Net ecosystem exchange of CO_2 (NEE), driven strongly by GPP during the growing season, shows a symmetrical diurnal cycle peaking on average around solar noon at -0.6 mgC m^{-2} s^{-1}. NEE switched to a weak source during the night and showed less variability than the daytime flux. The solar zenith arc almost exactly mirrors the pattern of NEE, indicating the strong role of light on GPP and of GPP on NEE as well as ET (Fig. 6).

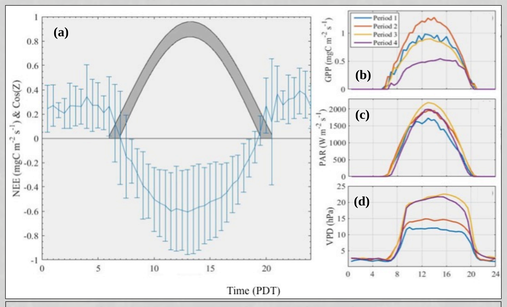

Fig. 7. Diurnal 30-minute averages of NEE with error bars representing +/- one standard deviation for the entire observation period as well as solar pattern (a). Diurnal ensemble 30-minute averages of (b) Gross Primary Production (GPP), (c) Photosynthetically active radiation (PAR) and (d) vapor pressure deficit (VPD) according to seasonal period.

5. Using greenness index from digital camera images to derive GPP

Daily midday images of the ecosystem (shown if Figs. 3 and 4) were sub-sampled, and pixel average greenness index was derived (GI= brightness values in green band / (blue + green + red brightness values).

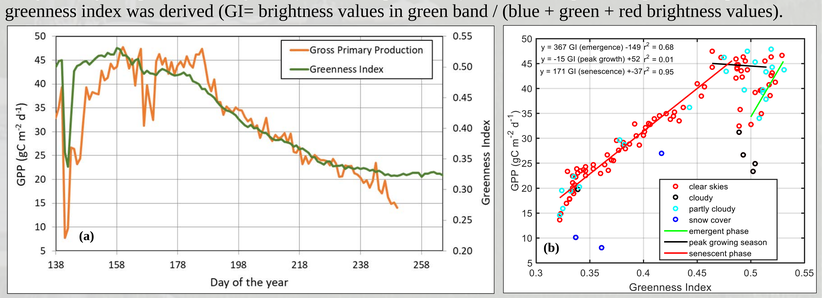

Fig. 8 (left) Seasonal trend of GPP and greenness index for the entire study period (a). (Center) Greenness index model with different sky conditions. The parameters for the combined model validation were as follows: N = 101, r^2 = 0.96, slope = 0.96, y-intercept = 1.2 model efficiency coefficient = 0.96, and root mean squared error = 1.9 gC m^{-2} d^{-1}.

6. Estimating annual CO_2 budget of Loney meadow

The annual CO_2 budget for Loney Meadow was estimated to be a sink of **-222 gC m^{-2} y^{-1}** in 2016. A linear regression model was used to extrapolate GPP and Re from Periods 1 and 4 to estimate remaining unmeasured snow-free days, and assuming a respiration rate of 1 gC m^{-2} d^{-1} during the snow covered (Wohlfart et al. 2008).

ACKNOWLEDGEMENTS

We would like to thank: Rachel Hutchinson and South Yuba River Citizens League (SYRCL) for continued research support and collaboration at Loney; the U.S. Forest Service for permitting access to the site; the Jean Vance Scholarship for funding; Quentin J. Clark for field support; and Suzanne Maher for helping with data analysis and guidance at all stages of this project.

REFERENCES

Loheide II, S. P., Deitchman, R. S., Cooper, D. J., Wolf, E. C., Hammersmark, C. T., & Lundquist, J. D. 2009. A framework for understanding the hydroecology of impacted wet meadows in the Sierra Nevada and Cascade Ranges, California, USA. *Hydrogeology Journal*, *17*(1), 229-246.

Viers, JH, SE Purdy, RA Peek, A Fryjoff-Hung, NR Santos, JVE Katz, JD Emmons, DV Dolan, and SM Yarnell. 2013. Montane Meadows in the Sierra Nevada: Changing Hydroclimatic Conditions and Concepts for Vulnerability Assessment. Center for Watershed Sciences Technical Report (CWS-2013-01), University of California, Davis. 63 ppd.

Wohlfahrt, Georg, Albin Hammerle, Alois Haslwanter, Michael Bahn, Ulrike Tappeiner, and Alexander Cernusca. "Seasonal and inter-annual variability of the net ecosystem CO2 exchange of a temperate mountain grassland: Effects of weather and management." *Journal of Geophysical Research: Atmospheres* 113, no. D8 (2008).